Physica C 235-240 (1994) 2765-2766
North-Holland

PHYSICA C

Surface Currents and Bulk Pinning in $Bi_2Sr_2CaCu_2O_8$

D. Majer,[a] E. Zeldov,[a] M. Konczykowski,[b] V. B. Geshkenbein,[c,a] A. I. Larkin,[c,a] L. Burlachkov,[d] V. M. Vinokur,[e] N. Chikumoto[f].
[a]Weizmann Institute of Science, 76100 Rehovot, Israel. [b]Laboratoire des Solides Irradies, Ecole Polytechnique, 91128 Palaiseau, France. [c]L. D. Landau Institute for Theoretical Physics, 117940 Moscow Russia. [d]Physics Department, Bar-Ilan University, 52900 Ramat-Gan, Israel. [e] Argonne National Laboratory, Argonne, IL 60439, USA. [f] University of Tokyo, Bunkyo-ku, Tokyo 113, Japan.

The mechanisms giving rise to the irreversibility line (IL) in the phase diagram of $Bi_2Sr_2CaCu_2O_8$ and the mechanism behind the second maximum in the magnetization loops were determined using a novel Hall-sensor array. The IL is caused by bulk pinning at lower temperatures and by irreversible shielding currents above 22K. The second maximum is caused by vortex lattice melting, taking place at the same local magnetic induction B_m throughout the sample.

The phase diagram of BSCCO in the mixed state was determined using a novel two-dimensional-electron-gas Hall-sensor array in temperature range of 17K to 92K. The array used in the reported study consisted of 11 in-line sensors of $10\mu m \times 10\mu m$ active area with $10\mu m$ separation and sensitivity better than 0.1 Gauss. A high quality $15\mu m$ thick BSCCO single crystal was attached to the array surface. The center of the sample was aligned with the array so that seven sensors (5 through 11) probed the induction along the width of the crystal and sensors 1 through 4 measured the edge field outside the sample. The crystal was zero field cooled and the constant-temperature magnetization loops in applied field $H_a||c$ axis were measured.

We believe two mechanisms determine the irreversibility line (IL) in BSCCO. One mechanism is bulk pinning causing the IL at $T < 22$K. The other, at higher temperatures, is the onset of irreversible shielding currents at $H_a \leq H_{IS}(T)$ [1]. In Fig. 1a, experimental magnetic field profiles at 22K are shown. The profiles are Bean-like [2], suggesting that bulk pinning is the main mechanism present. The profiles at 74K (Fig. 1b), are very different from Bean-like profiles and are the result of irreversible shielding currents. A more accurate way to determine the source of the IL is to look at the direction of the induction gradient $dB_z(x)/dx$ vs. H_a loops. The loops have *anti-clockwise* direction when bulk pinning is present and *clockwise* direction when surface currents are

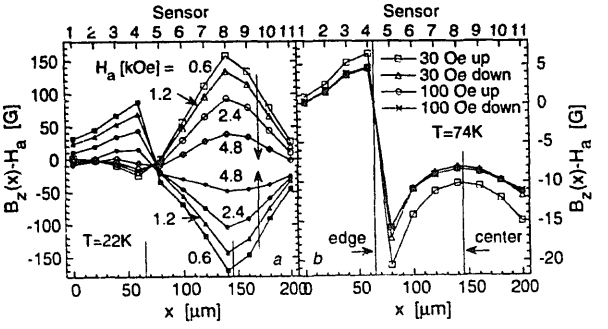

Figure 1. Magnetic profiles inside and outside BSCCO crystal. At 22K Bean type profiles are observed (a). At 74K very different, bell-shaped profiles are the result of irreversible shielding currents (b).

dominant [3]. $H_{IL}(T)$ was checked independently by analyzing the magnetization loops using the integrated induction of all the sensors. The irreversibility line coincides with $H_{IS}(T)$ at intermediate and high temperatures and with the bulk depinning line $H_{dp}(T)$ at low temperatures.

At $T < 22$K bulk pinning governs the shape of the magnetization loop in the entire field range; no distinct second peak is obtained and IL is due to bulk pinning. At intermediate temperatures a clear second peak is observed below which the bulk critical current is negligible.

In the region of the second maximum we observe a very sharp transition of J_c with respect to B, which we identify as vortex lattice melting at $B_m(T)$. The measured magnetic field profiles in the vicinity of $B_m(T)$ are shown in Fig. 2.

SSDI 0921-4534(94)01948-7

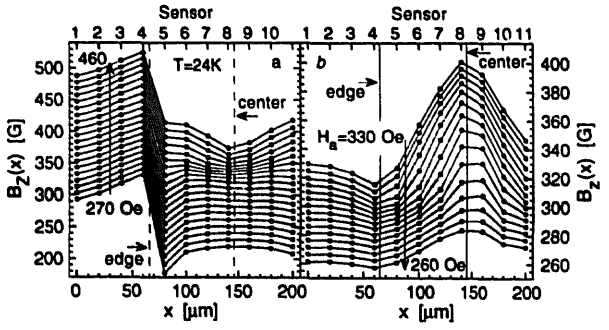

Figure 2. Experimental magnetic field profiles in ascending (a) and descending (b) magnetic fields at 24K. Solidification nucleates at the sample center (a) and melting starts at sample edges (b).

In ascending field, solidification of the vortex lattice starts at the center of the sample where B_m is reached first and the solid region expands towards the sample edges (Fig. 2a). In descending magnetic field (Fig. 2b), the melting front starts at the sample edges and moves towards the middle of the sample. At high fields large slopes of $B_z(x)$ are observed due to the presence of large critical currents. As $B_z(x)$ drops below $\sim$ 320 G at various locations inside the sample, a sharp drop in the local current density occurs which results in a significant reduction of the local induction gradient. At lower fields, bulk currents are negligible and dome-shaped profiles are obtained. In more detailed analysis [3] of $dB_z(x)/dx$, one observes a sharp melting transition taking place at the same local induction $B_z(x) = B_m$. This melting occurs at various values of H_a for various locations inside the sample which is one of the reasons for a much broader second peak observed in integrated magnetization measurements.

Fig. 3 shows the derived phase diagram of BSCCO in a wide field and temperature range. Since on the descending branch the shielding currents have a very weak field dependence we may obtain the high field depinning line $B_{dp}(T)$ by determining the upturn point of the induction gradient. At low temperatures we observe a crossover of $B_{dp}(T)$ and $H_{IS}(T)$ and hence $H_{IL}(T) = B_{dp}(T)$ for $T < 22$K. The sharp split of $B_{dp}(T)$ and $B_m(T)$ and the temperature dependence of the melting line suggest that the observed $B_m(T)$ is the low field reentrant melting.

In the 25K to 50K temperature range both the penetration field $H_p(T)$ and $H_{IL}(T)$ show an exponential temperature dependence which is consistent with thermal activation of the vortices over a Bean-Livingston surface barrier [4]. At $T > 60K$ $H_p(T)$ and $H_{IS}(T)$ follow a linear temperature dependence. Such behavior is consistent with the presence of geometrical barriers [1,3]. At lower temperatures the observed upturn of $H_p(T)$ and $H_{IL}(T)$ is the result of a significant bulk pinning.

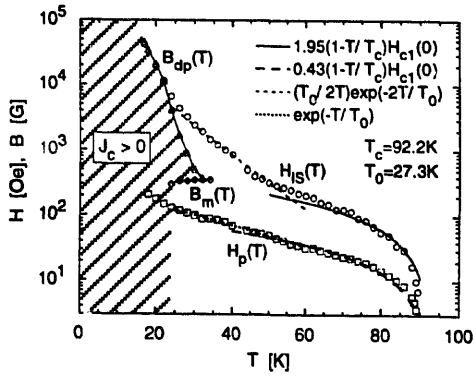

Figure 3. Phase diagram of $Bi_2Sr_2CaCu_2O_8$.

This work was supported by the Israeli Ministry of Science and the Arts, by the Philip M. Klutznick Fund, by MINERVA foundation, and by France-Israel cooperation program PICS 112. VMV acknowledges the support through US Department of Energy, BES-Materials Sciences, under contract No. W-31-109-ENG-38.

REFERENCES

1. E. Zeldov, A.I. Larkin, V.B. Geshkenbein, M. Konczykowski, D.Majer, B. Khaykovich, V.M. Vinokur, and H. Shtrikman (unpublished).
2. C. P. Bean, Phys. Rev. Lett. **8**, 250 (1962); E. Zeldov, J.R. Clem, M. McElfresh, and M. Darwin, Phys. Rev.B **49**, 9802 (1994); E.H. Brandt and M.V. Indenbom, Phys. Rev. B **48**, 12893 (1993); A.I. Larkin and Yu.N. Ovchinnikov, Zh. Eksp. Teor. Fiz. **61**, 1221 (1971) [Sov. Phys. JETP **34**, 651 (1972)].
3. E. Zeldov, D. Majer, M. Konczykowski, A. I. Larkin, V. M. Vinokur, V. B. Geshkenbein, N. Chikumoto, and H Shtrikman (unpublished).
4. C.P. Bean and J.D. Livingston, Phys. Rev. Lett. **12**, 14(1964); L. Burlachkov, V.B. Geshkenbein, A.E. Koshelev, A.I. Larkin, and V.M. Vinokur (unpublished).